Identifying plant species using architectural features of leaf microscopy images

Florindo, Joao Batista; Bruno, Odemir Martinez; Rossatto, D R; Kolb, R M; Gomez, M C; Landini, Gabriel

DOI:
10.1139/cjb-2015-0075

Identifying Plant Species Using Architectural Features of Leaf Microscopy Images

J. B. Florindo *[1], O. M. Bruno[2], D. R. Rossatto[3], R. M. Kolb[4], M. C. Gómez[5], and G. Landini[6]

[1]*São Carlos Institute of Physics, University of São Paulo, PO Box 369, 13560-970, São Carlos, SP, Brazil, email: jbflorindo@gmail.com*

[2]*São Carlos Institute of Physics, University of São Paulo, PO Box 369, 13560-970, São Carlos, SP, Brazil, email: bruno@ifsc.usp.br*

[3]*Departament of Biology, Faculty of Agrarian and Veterinary Sciences, Univ Estadual Paulista, Jaboticabal, SP Brazil, email:drrossatto@gmail.com*

[4]*Department of Biological Sciences, Faculty of Sciences and Letters, Univ Estadual Paulista Júlio de Mesquita Filho, UNESP, Brazil, email: rosanakolb@hotmail.com*

[5]*Department of Physics, Faculty of Biochemistry and Biological Sciences, National University of Littoral, Santa Fe, Argentina, email: mcgpna@gmail.com*

[6]*Oral Pathology Unit, School of Dentistry, University Of Birmingham, Birmingham, United Kingdom, email: G.Landini@bham.ac.uk*

*Corresponding author

Abstract

This work proposes an analytical method to identify plant species based on microscopy images of the midrib cross-section of leaves. Unlike previous shape-based approaches based on the individual shape of external contours and cells, an architectural analysis is proposed, where the midrib is semi-automatically segmented and partitioned into histologically relevant structures composed of layers of cells and vascular structures. Using a sequence of morphological operations, a set of geometrical measures from the cells in each layer is extracted to produce a vector of features for species categorization. The method applied to a database containing 10 species of plants from the Brazilian *flora* achieved a success rate of 91.7%, outperforming other classical shape-based approaches published in the literature.

Keywords— Automatic Species Identification, Image Analysis, Morphological Features

1 Introduction

The categorization of plants into species is an important taxonomical task; it provides meaningful information about particular characteristics of a plant, which can be used in the context of biodiversity and environmental relations with other species.

Plant identification is an old problem and, classically it has been based on conventional visual characterisation of plant morphology. It is only recently that computer-based analyses have been used for this purpose (Rossatto et al., 2011; Sá Junior et al., 2011; Florindo et al., 2014; Silva et al., 2014). Computational methods are particularly interesting because they enable a more precise identification of plant leaves, especially when leaves from different species are too similar to each other and the conventional morphological features are not sufficient for their discrimination (Bruno et al., 2008; Backes et al., 2009; da Silva et al., 2015; Florindo et al., 2014). This is especially important in situations where, for example, reproductive structures are not easily obtainable like plants in vegetative phase.

Among the computational methods proposed, those using information from the leaves have become very popular, mostly because leaves can be easily found at any time. Image analysis has proven to be a powerful tool in the description of these structures (Florindo et al., 2014). Leaves are diverse and complex structures in terms of anatomy and morphology (Evert, 2006) and modern computational approaches can extract large amount of useful information from them.

Most analyses of leaf images use macroscopic features such as leaf contour and venation distribution, among others (Backes et al., 2009; Bruno et al., 2008). More recently, the analysis of microscopic features has been a subject of investigation, using images from midrib cross-sections (Silva et al., 2014). Those studies, however, used approaches to characterise leaf structure externally or internally, as indivisible elements without taking into consideration the relations between their parts (for instance, cells and vascular spaces observed in cross-sections).

Here we propose a taxonomic analysis of plant leaves, based on quantifying the architecture of the midrib as observed in microscopical cross-sections. More specifically, the midrib is characterised using adjacent layers of cells and vascular spaces. Visually, it can be noticed that cells and vascular spaces (represented in analytical terms by pixel regions called 'v-cells' or 'virtual cells') are arranged in a seemingly hierarchical order or layers such that they appear to exhibit characteristic morphological features at various depths from the leave surface. The analysis, therefore, is aimed at computing various morphological descriptors of this structural organisation (e.g. v-cell area, perimeter, Feret diameter and others) forming those layers. Those layer descriptors are averaged and the resulting set of features submitted first to a Karhunen-Loève transform to reduce the data dimensionality and then to a learning machine algorithm to classify the cases into different plant species.

When this novel approach was applied to a database of plants from the

Brazilian *flora*, 91.7% of the samples were successfully identified, suggesting that the proposed method might be useful for taxonomic identification. The results also suggest that the organization of v-cells within a leaf might provide useful descriptors for defining architectural metrics to investigate and compare how species might be morphologically related.

2 Material

The material analysed is composed of 10 species from the Cerrado vegetation in Brazil. Table 1 shows the name of the collected species (six samples per species). More details about the database can be found in da Silva et al. (2015)[1]. The central part of the leaf (including the midrib) was fixed in FAA (Formalin-Acetic Acid-Alcohol) 70 for 48 hours (Johansen, 1940), then dehydrated in an ethanol series and embedded in paraffin. Afterwards, 8μm-thick cross-sections were cut, rehydrated and stained with Astra blue and basic fuchsin, dehydrated and finally mounted with Entellan. The images of midribs were captured with a 10x objective lens, in a trinocular Axio Lab A1 microscope coupled to a digital Axiocam ICc 1 camera (Zeiss, Germany). After images were captured, the region containing the midrib was manually separated from the background.

Table 1: Plant species in the database analysed here (six samples per species).

Family	Species
Anacardiaceae	*Anacardium humile* A. St.-Hil.
Annonaceae	*Annona crassiflora* Mart.
Aristolochiaceae	*Aristolochia galeata* Mart. & Zucc.
Bignoniaceae	*Arrabidaea brachypoda* Bur
Apocynaceae	*Aspidosperma subincanum* Mart.
Asteraceae	*Baccharis salzmannii* DC.
Fabaceae	*Bauhinia pulchella* Benth.
Fabaceae	*Bauhinia ungulata* L.
Malpighiaceae	*Banisteriopsis stellaris* (Griseb.) B.Gates
Malpighiaceae	*Byrsonima laxiflora* Griseb.

3 Proposed method

The method proposed here consists of 4 steps: pre-processing of the cross-section, segmentation of v-cells, labelling of layers of v-cells, and extraction of features from each layer.

[1]The database is available for downloading at https://dataverse.harvard.edu/dataset.xhtml?persistentId = doi:10.7910/DVN/KDZVUM

3.1 Pre-processing

First, the midrib region of the section is manually selected (by the operator) and separated from the mesophyll region. The midrib image (Figure 1a) was then preprocessed for noise suppression and background illumination by applying the following operation:

- **Gaussian Blur** - The original colour image is converted to grey-levels, inverted and convolved with a Gaussian filter with radius 5 around each pixel to attenuate some noise and outliers by smoothing (Figure 1b).

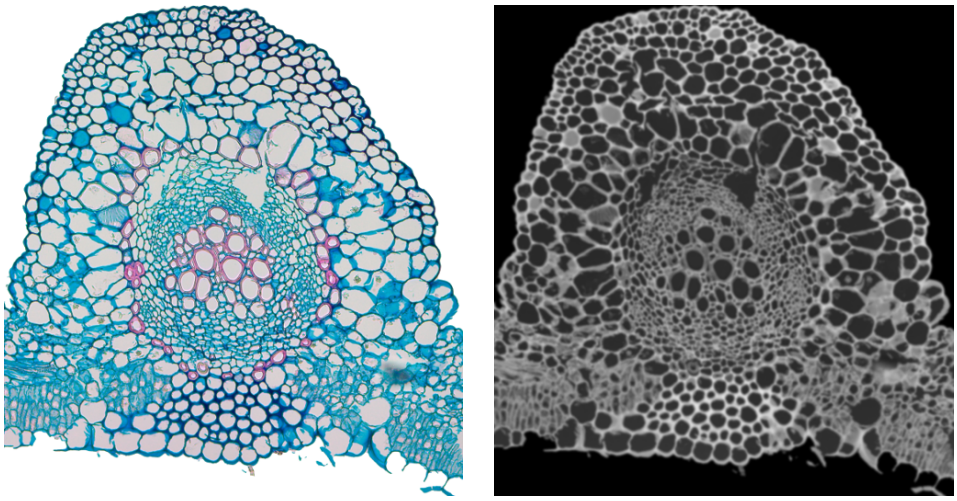

(a) (b)

Figure 1: Pre-processing operation. (a) Original image. (b) Grey-level inversion and Gaussian blurring.

These steps were carried out in ImageJ[2]. Figure 1 shows the result image after processing.

3.2 Morphological segmentation

The morphological segmentation of grey-level images, used here and presented in Vincent and Dougherty (1994), is based on the watershed transform which relies on detecting 'catchment basins' on the grey-level image, when considering that pixel greyscale values represent the 'height' of the greyscale function. The catchment basins are those regions where imaginary drops of water falling over the image would tend to accumulate. The borders where the different catchment basins meet are called *watershed lines*.

[2]ImageJ is a public domain program for image processing written by W. Rasband, available at http://imagej.nih.gov.

Depending on application, the watershed lines are computed from the image itself, or from its gradient (so the watershed lines tend to be located at the edges of image objects). Here we exploit a mathematical morphology approach and use the Beucher's gradient, defined for image I as

$$grad(I) = (I \oplus B) - (I \ominus B), \tag{1}$$

where B is a unitary ball and $\oplus$ and $\ominus$ stand for the morphological dilation and erosion, respectively.

The extraction of watershed lines from the greyscale gradient sometimes tends to over-segment the image (i.e. produces too many basins). The method described in Vincent and Dougherty (1994) seeks to avoid this by redefining the gradient through a morphological grey-level reconstruction driven by a marker image. Thus given the gradient image $J = grad(I)$ and the marker image M, a new reconstructed gradient J' can be computed.

First, for every pixel p, J and M are transformed into J^* and M^* by

$$J^*(p) = \begin{cases} h_{min} \text{ if } M(p) = 1 \\ J(p) \text{ otherwise,} \end{cases} \tag{2}$$

and

$$M^*(p) = \begin{cases} h_{min} \text{ if } M(p) = 1 \\ h_{max} \text{ otherwise,} \end{cases} \tag{3}$$

where h_{min} and h_{max} are chosen such that $\forall p, h_{min} < J(p), h_{max} > J(p)$.

At this point, it is important to define the procedure called dual grey-scale reconstruction. This procedure is not exactly straightforward and so it is explained next using simpler concepts. The first concept is the n^{th} geodesic dilation $\delta_X^n(Y)$ of a set $Y \subseteq X$. In terms of morphological operations, for $n = 1$:

$$\delta_X^1(Y) = (Y \oplus B) \cap X, \tag{4}$$

and $\delta_X^n(Y)$ is defined recursively:

$$\delta_X^n(Y) = \delta_X^1(\delta_X^{n-1}(Y)). \tag{5}$$

Based on that, the reconstruction $\rho_X(Y)$ is given by

$$\rho_X(Y) = \lim_{n \to \infty} \delta_X^n(Y). \tag{6}$$

In practice, only a few steps are necessary to achieve the expected reconstruction.

Given two grey-scale images I and J defined over the same domain, assuming discrete grey-levels $\{0, 1, \cdots, N\}$, and satisfying $\forall p, J(p) \geq I(p)$, the reconstructed image of I *from* J is given by

$$\rho_I^*(J)(p) = N - \rho_{N-I}(I - J), \tag{7}$$

where ρ is the reconstruction defined by

$$\rho_I(J)(p) = \max\{k \in [0, N] | p \in \rho_{T_k(I)}(T_k(j))\}, \tag{8}$$

and $T_k(I)$ is the set of pixels p such that $I(p) \geq k$.

Finally, after the above definition, J' is provided by a dual grey-level reconstruction:

$$J'(p) = \rho^*_{J^*}(M^*). \tag{9}$$

The final step of the segmentation is to extract the watershed lines of J'.

More details, rationale and illustrated examples can be found in Vincent and Dougherty (1994). In terms of computational implementation, an imageJ plug-in[3] was used, with a tolerance threshold of 10. Figure 2 illustrates how the v-cells are identified by the method.

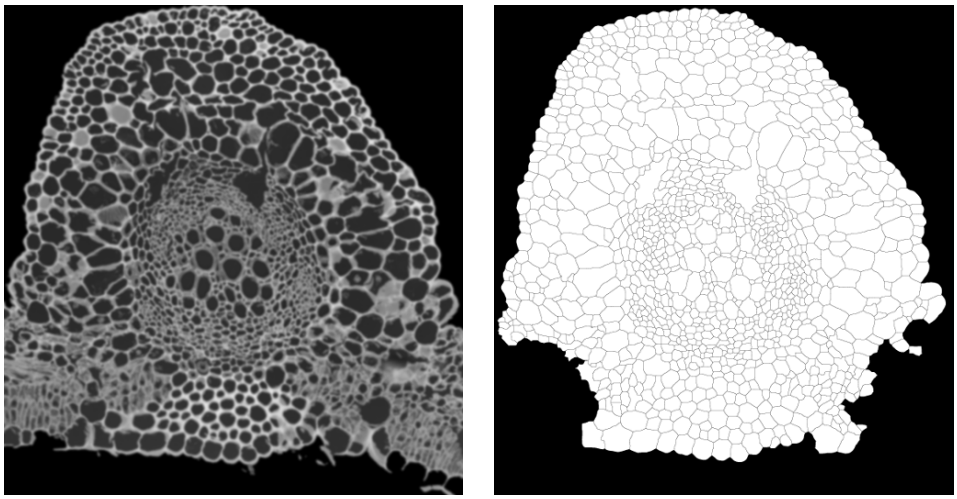

(a) (b)

Figure 2: Morphological segmentation of the cross-section cells. (a) Preprocessed image (resulting from Figure 1). (b) Morphological segmentation.

3.3 Extraction of layers

The tissue structure in the cross-sections has a relatively symmetrical arrangement, resembling layers of cells and vascular spaces with similar properties (size, shape) across the species studied.

The v-cell layers are sets of v-cells that fulfill specific adjacency relations and these can be computed using the algorithm described by Landini and Othman (2003).

[3]Available at http://fiji.sc/Morphological_Segmentation.

The first step in this procedure is to identify the outmost external layer. This is achieved by identifying those v-cells adjacent to the background region. The v-cells in the segmented cross-section C are merged into C', by applying a closing operation:

$$C' = (C \oplus S) \ominus S, \tag{10}$$

where S is a 3×3 structuring element.

The background is then dilated, which gives rise to a region R of intersection with the v-cells, computed using

$$R = C \wedge \bar{C}' \oplus S, \tag{11}$$

where $\bar{C}'$ is the binary inversion of C'.

The first layer is obtained by the binary reconstruction of C from R and is labelled as 1. Once the first layer has been identified, the remaining layers are computed by considering the previous layer as the background and applying two consecutive dilations in Equation 11 (the first one fills the gap between the v-cells, the second provides the overlap with not-yet-labelled v-cells and which is used by the reconstruction operation to identify the next adjacent layer). The layers are increasingly labelled 2, 3, 4, and so on. Here, such labelling procedure was applied in two directions (from dorsal to ventral surface and vice-versa) and the minimum of these labels define the layers from the closest free surface of the leaf.

More details and a pseudo-code can be found in Landini and Othman (2003). Figure 3 shows the layers identified in the segmented image.

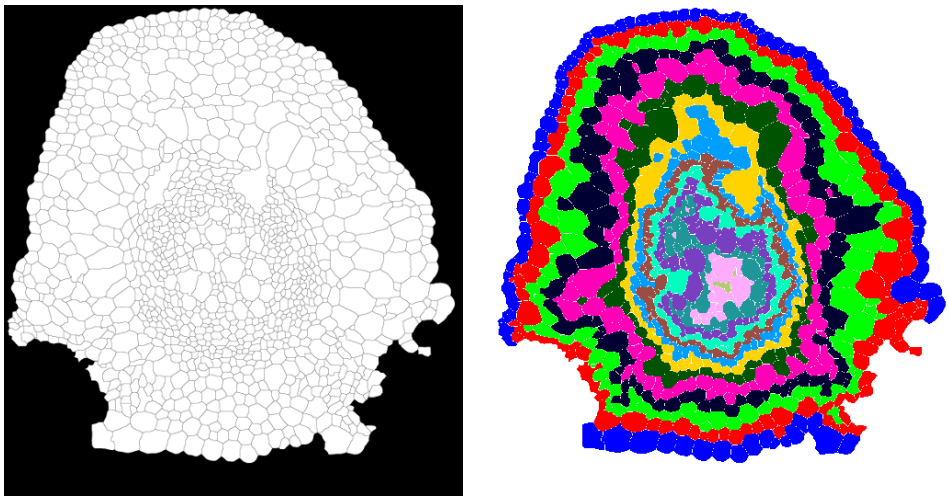

(a) (b)

Figure 3: External layers highlighted in different colours over the segmented image. (a) Segmented image (resulting from Figure 2). (b) Extracted layers.

3.4 Extraction of layer features

The final step in the proposed method was to compute the features of the v-cells, according to the layer where they were located.

A straightforward and efficient way of representing layer features is to calculate the mean $\mu_L^M(x)$ of the measure M over the cells x in the layer L. A potential problem of using the mean is that segmentation inaccuracies can result in very large or small v-cells which are not strictly cellular or vascular structures, e.g. empty spaces and/or over/under-segmented regions. To minimise this, outliers with areas 95% larger or smaller than the mean were removed and $\mu_L^M(x)$ was computed in two steps. In the first an auxiliary mean $m_L^M(x)$ is computed by

$$m_L^M(x) = \frac{1}{N} \sum_{x \in L} M(x) \tag{12}$$

and from that $\mu_L^M(x)$ is obtained through

$$\mu_L^M(x) = \frac{1}{N} \sum_{x \in L'} M(x), \tag{13}$$

where $L' = \{x | \|M(x) - m_L^M(x)\| < 0.95\text{sup}(\|M(x) - m_L^M\|)\}$.

For M, 25 different measures were employed. They were inspired by (Landini, 2006, 2008) and are listed in Table 2. A complete description of each measure can be found in Landini (2006, 2008).

Table 2: Measures M computed for each v-cell.

Perimeter	PerimEquivD
Area	EquivEllipseAr
MinR	Compactness
MaxR	Solidity
Feret	Concavity
Breadth	Convexity
CHull	Shape
CArea	RFactor
MBCRadius	ModRatio
AspRatio	Spericity
Circ	ArBBox
Roundness	Rectang
AreaEquivD	

Finally, all the values of μ_L^M, for each layer L and each measure M, were concatenated to create a vector of features. This results in a large set of features, depending on the number of layers and the number of measures considered in each layer. To address this and produce results comparable to other classification methods, the concatenated features were submitted to a Karhunen-Loève transform (also called Principal Component Analysis or PCA) to reduce the

data dimensionality. The most significant scores were used in the next machine learning step. Figure 4 shows a simple diagram of the method described for the analysis of a leaf cross-section.

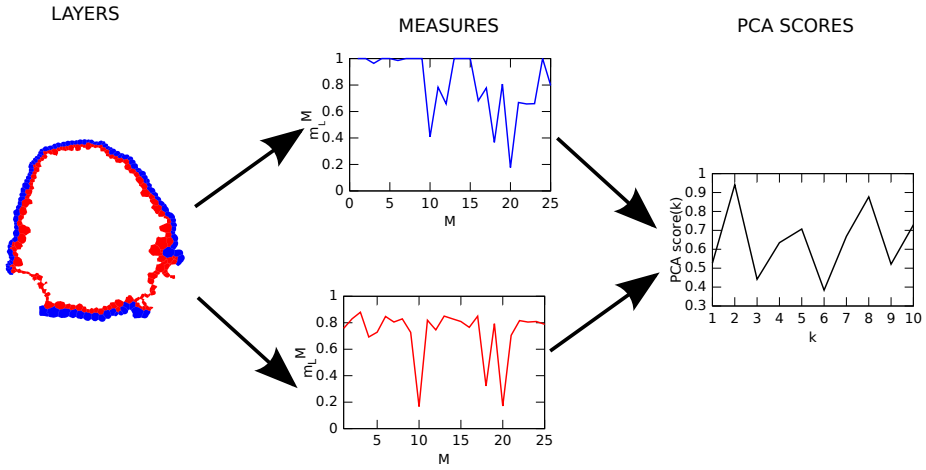

Figure 4: A basic diagram of the proposed method. From left to right, the layered cross-section, the average measures estimated over two layers and the resulting concatenation after Karhunen-Loève reduction.

3.5 Assessment

The categorization of species was carried out by means of a learning machine method using the PCA scores as input. A cross-validation strategy was employed, where the samples were split into training and testing sets, following a 10-fold procedure. This consisted of dividing the samples into 10 subsets with similar sizes and in each round nine subsets were used for training and the remaining one for testing (as described in Duda and Hart (1973)). The categorization was finally accomplished by a Linear Discriminant Analysis (LDA) (Duda and Hart, 1973), following similar approaches used in other reported plant image analyses (Backes et al., 2009; Florindo et al., 2014).

We compared our results to those from shape-based methods previously reported in the literature, namely, Multiscale Fractals (Bruno et al., 2008) (using the entire multiscale curve), Invariant Moments (Hu, 1962) (7 moments) as well as a classification based on the measures computed over the v-cells (irrespective of the layers where they were located). Those methods were implemented following the published descriptions to analyse the contour of the v-cells. The multiscale fractal descriptors were computed on the shapes of v-cells as the object of interest, whereas the moment descriptors were averaged over all the v-cells. To make results comparable across methods in terms of descriptor numbers, the extracted feature vectors were submitted to the Karhunen-Loève transform and the first n scores (up to a maximum of 100) were used in the assessment.

4 Results and discussion

Table 3 shows the success rates obtained by the proposed method and other published approaches. Our method outperforms the direct use of v-cells and all the others by at least 5%, showing how the architectural analysis is able to provide additional information on the structural morphology of leaf cross-section. We also investigated whether unbalanced sized groups of species in the database made significant differences to the results. We repeated the analysis using all the samples in the database (total $n = 96$, instead of six samples per species, $n = 60$) and found that the correct rate of identification for the proposed method was practically the same (91.8%) and this result was also higher than for the "Cells" approach (87.3%).

Table 3: Correctness rate obtained by the proposed method, in comparison with other shape-based approaches in the literature.

Method	Correctness rate (%)	Number of features
Invariant moments	46.7±0.2	4
Multiscale fractal	68.3±0.2	3
Cells	86.7±0.1	19
Proposed method	91.7±0.1	12

The results show that the analysis of midrib architecture is useful to describe its complex structure in cross-sections and highlights the importance of micro-anatomy in plant taxonomy, in particular how the cellular structures are assembled following a characteristic order and pattern, which appears to be characteristic and conserved in samples of the same species, but statistically different across species.

There are still some challenges that need to be resolved to fully automate this type of analysis. Two of these are the spatial orientation of the specimen within the image frame and the identification of the midrib section (the region of interest), which currently require operator input.

5 Conclusions

This work presented a new type of analysis for the identification of plant species based on microscopical images of midrib cross-sections. Instead of the classical shape-based analysis focused on leaf contours or individual cells, we have the partitioning of the midrib cross-sections into histologically relevant structures (cell and vascular spaces) and their spatial organization (layers). This provided a level of description that machine learning procedures were able to exploit for the identification of plant species.

The performance of the method was tested using a database of plants from the Brazilian *flora* (da Silva et al., 2015) and compared with previous approaches published in the literature. Our method achieved a success rate of 91.7% over a set of 10 plant species. This is an encouraging result, which is higher than the

performance of other computational approaches to this problem. Furthermore, this also gives some idea of how a layer-wise analysis can improve a shape-based analysis of this type of material, suggesting a more in-depth investigation in the future.

Acknowledgments

Odemir Martinez Bruno gratefully acknowledges the financial support of CNPq (National Council for Scientific and Technological Development, Brazil) (Grant Nos. 308449/2010-0 and 473893/2010-0) and FAPESP (Grant No. 2011/01523-1). Joao Batista Florindo acknowledges support from FAPESP (The State of São Paulo Research Foundation) (Grant No. 2013/22205-3). Gabriel Landini acknowledges support from the Engineering and Physical Sciences Research Council (UK) (Grant No. EP/M023869/1). Rosana Marta Kolb acknowledges the financial suport of Fapesp (Grant No. 2011/23112-3).

References

Backes, A. R., Casanova, D., and Bruno, O. M. (2009). Plant leaf identification based on volumetric fractal dimension. *International Journal of Pattern Recognition and Artificial Intelligence*, 23(6):1145–1160.

Bruno, O. M., de Oliveira Plotze, R., Falvo, M., and de Castro, M. (2008). Fractal dimension applied to plant identification. *Information Sciences*, 178(12):2722–2733.

da Silva, N. R., Florindo, J. a. B., Gómez, M. C., Rossatto, D. R., Kolb, R. M., and Bruno, O. M. (2015). Plant identification based on leaf midrib cross-section images using fractal descriptors. *PLoS ONE*, 10(6):e0130014.

Duda, R. O. and Hart, P. E. (1973). *Pattern Classification and Scene Analysis*. Wiley, New York.

Evert, R. F. (2006). *Esau's Plant Anatomy, Meristems, Cells, and Tissues of the Plant Body: their Structure, Function, and Development*. Wiley, Hoboken.

Florindo, J., Silva, N., Romualdo, L., Silva, F., Luz, P., Herling, V., and Bruno, O. (2014). Brachiaria species identification using imaging techniques based on fractal descriptors. *Computers and Electronics in Agriculture*, 103:48–54.

Hu, M.-K. (1962). Visual pattern recognition by moment invariants. *Information Theory, IRE Transactions on*, 8(2):179–187.

Johansen, D. A. (1940). *Plant microtechnique*. McGraw-Hill Book Company, inc., New York/London.

Landini, G. (2006). Quantitative analysis of the epithelial lining architecture in radicular cysts and odontogenic keratocysts. *Head & Face Medicine*, 2(1).

Landini, G. (2008). Advanced shape analysis with imagej. In *Proceedings of the Second ImageJ User and Developer Conference, Luxembourg, 6-7 November, 2008*, pages 116–121.

Landini, G. and Othman, I. E. (2003). Estimation of tissue layer level by sequential morphological reconstruction. *Journal of Microscopy*, 209(2):118–125.

Rossatto, D. R., Casanova, D., Kolb, R. M., and Bruno, O. M. (2011). Fractal analysis of leaf-texture properties as a tool for taxonomic and identification purposes: a case study with species from neotropical *Melastomataceae* (*Miconieae tribe*). *Plant Systematics and Evolution*, 291(1-2):103–116.

Sá Junior, J., Backes, A., Rossatto, D., Kolb, R., and Bruno, O. (2011). Measuring and analyzing color and texture information in anatomical leaf cross sections: an approach using computer vision to aid plant species identification. *Botany (Ottawa. Print)*, 89(1):467–479.

Silva, N. R., Florindo, J. B., Gómez, M. C., Kolb, R. M., and Bruno, O. M. (2014). Fractal descriptors for discrimination of microscopy images of plant leaves. *Journal of Physics: Conference Series*, 490(1):012085.

Vincent, L. and Dougherty, E. (1994). Morphological segmentation for textures and particles. In Dougherty, E., editor, *Digital Image Processing Methods*. Marcel-Dekker, New York.